A D- and ^{15}N-rich micrometer-sized aggregate of organic matter in a xenolithic clast from the Zag ordinary chondrite

Yoko Kebukawa[1]*, Motoo Ito[2], Michael E. Zolensky[3], Zia Rahman[4], Hiroki Suga[5], Aiko Nakato[6], Queenie H. S. Chan[3†], Marc Fries[3], Yasuo Takeichi[7], Yoshio Takahashi[8], Kazuhiko Mase[7], and Kensei Kobayashi[1]

*Corresponding author: kebukawa@ynu.ac.jp

[1]Faculty of Engineering, Yokohama National University, 79-5 Tokiwadai, Hodogaya-ku, Yokohama 240-8501, Japan

[2]Kochi Institute for Core Sample Research, JAMSTEC, B200 Monobe, Nankoku, Kochi 783-8502, Japan

[3]ARES, NASA Johnson Space Center, 2101 NASA Parkway, Houston, TX 77058, USA

[4]Jacobs, NASA Johnson Space Center, Houston, TX 77058, USA

[5]Department of Earth and Planetary Systems Science, Hiroshima University, Kagamiyama, Higashi-Hiroshima, Hiroshima 739-8526, Japan

[6] Graduate School of Science, Kyoto University, Kitashirakawa Oiwake-cho, Sakyo-ku, Kyoto 606-8502, Japan

[7]Institute of Materials Structure Science, High-Energy Accelerator Research Organization (KEK), 1-1 Oho, Tsukuba, Ibaraki 305-0801, Japan

[8]Department of Earth and Planetary Science, The University of Tokyo, Hongo, Bunkyo-ku, Tokyo 113-0033, Japan

[†]Current address: Department of Physical Sciences, The Open University, Walton Hall, Milton Keynes, MK7 6AA, UK

Summary

The nature and origin of extraterrestrial organic matter are still under debate despite the significant progress in the analyses and experimental approaches in this field over the last five decades. Xenolithic clasts are often found in a wide variety of meteorite groups[1-8], some of which contain exotic organic matter (OM). The Zag meteorite is a thermally-metamorphosed H ordinary chondrite. It contains a primitive xenolithic clast that has been proposed to have originated from Ceres[9-11], which was accreted to the Zag host asteroid after metamorphism. The cm-sized clast contains abundant large carbon-rich (mostly organic) grains or aggregates up to 20 μm[10-12]. Such large OM grains are unique among astromaterials with respect to the size. Here we report organic and isotope analyses of a large (~10 μm) aggregate of solid OM in the Zag clast. The X-ray micro-spectroscopic technique revealed that the OM has sp^2 bonded carbon with no other functional groups nor graphitic feature (1s-σ* exciton), and thus it is distinguished from most of the OM in carbonaceous meteorites. The apparent absence of functional groups in the OM suggests that it is composed of hydrocarbon networks with less heteroatoms, and therefore the OM aggregate is similar to hydrogenated amorphous carbon (HAC)[13-18]. The OM aggregate has high D/H and $^{15}N/^{14}N$ ratios, suggesting that it originated in a very cold environment such as the interstellar medium or outer region of the solar nebula, while the OM is embedded in carbonate-bearing matrix resulting from aqueous activities. Thus the high D/H ratio must have survived the extensive late-stage aqueous processing. It is not in the case for OM in carbonaceous chondrites of which the D/H ratio was reduced by the alteration via the D-H exchange of water[19]. It indicates that both the OM precursors and the water had high D/H ratios, similar to the water in Enceladus[20]. Our results support the idea that the clast originated from Ceres, or at least, a hydrovolcanically active body similar to Ceres, and further imply that Ceres

originally formed in the outer Solar System and migrated to the main belt asteroid region[21] as suggested by the "Grand tack" scenario[22].

Xenolithic clasts are present in a wide variety of meteorite groups[1-8]. These clasts have been protected in host meteorites that are typically more metamorphosed and thus are physically strengthened by thermal annealing via heating processes occurring prior to the incorporation of the clasts. Hence, such clasts can contain primitive and fragile materials that would not have survived parent body alteration processes and atmospheric entry. The Zag meteorite is a H3-6 chondrite which fell in Morocco on August 1998, and is known to contain xenolithic, fluid inclusion-bearing halite crystals and a centimeter-sized carbonaceous chondrite-like clast[1]. These clasts and halite crystals in the Zag meteorite have been proposed to be materials from dwarf planet 1/Ceres in light of their mineralogy and the orbital dynamics of a possible parent body[9,11]. The Zag clast consists of saponite, serpentine, Ca-Fe-Mg carbonates, Fe-Ni sulfides, magnetite, halite, minor olivine and pyroxene, as well as abundant large OM grains or aggregates up to 20 μm (Fig. 1), all consistent with formation on a large, aqueously active, carbonaceous body, e.g., Ceres[10,11,23]. Ceres' orbit crosses that of the proposed H chondrite parent body, asteroid 6/Hebe[9,24]. The current mean infall velocity of material transferred from Ceres to Hebe is approximately 1.20 to 1.38 km/s, although this transfer velocity could have been lower in the past[9]. This infall velocity is generally relatively low for transfer of material between inner Solar System bodies and thus survival of fragile material would be possible.

We analyzed the molecular structure and isotope chemistry of a focused ion beam (FIB) ultra-thin section obtained from an OM aggregate using scanning transmission X-ray microscopy (STXM) and nanoscale secondary ion mass spectrometry (NanoSIMS).

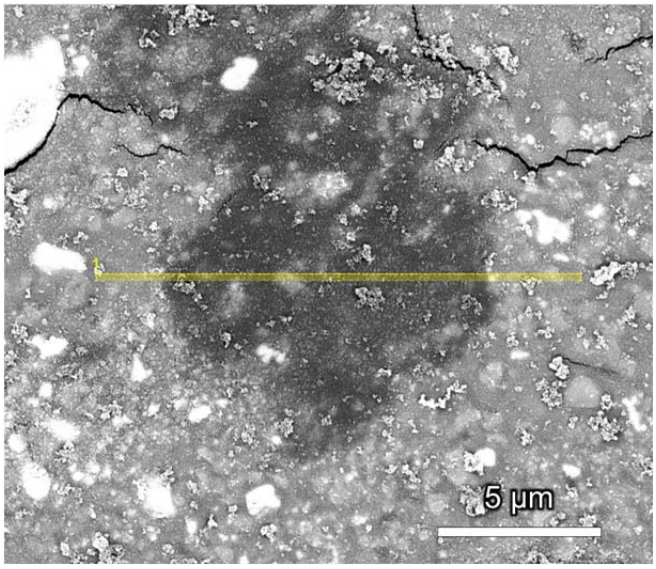

Fig. 1: Backscattered electron (BSE) image of a polished thin section of the organic aggregate (dark) in the carbonaceous clast in the Zag meteorite. FIB section was subsample from yellow region.

The FIB section obtained from the OM aggregate (Fig. 1) showed a large carbon-dominated area over 10 µm in width that corresponded to the OM aggregate (**Fig. 2**). A carbon X-ray absorption near edge structure (C-XANES) spectrum of the OM aggregate showed a peak at 284.8 eV that is assigned to sp^2 (aromatic) carbon (**Fig. 2**b,c in red). The surrounding matrix area showed a peak at 290.3 eV that is assigned to carbonates (CO_3) with some organic features at 284.8 eV, 286.3 eV (assigned to ketone [C=O]) and 288.5 eV (assigned to carboxyl/ester [(C=O)O]) (**Fig. 2**b,c in green). The C-XANES spectrum of the OM aggregate does not show

other peaks that are characteristic of insoluble organic matter (IOM) in primitive chondrites (e.g., C=O and (C=O)O indicating primitive OM in Murchison meteorite)[25], nor that in the thermally-metamorphosed meteorites (e.g., 1s-σ* exciton at 291.7 eV indicating graphene structures in the Allende meteorite)[26]. The C-XANES of the OM aggregate most resembles sp^2-rich hydrogenated amorphous carbon (HAC, also written as a-C:H) like material[13-18]. No detectable nitrogen features were observed in N-XANES spectra of the OM aggregate, probably due to low concentration of nitrogen, while matrix showed a small peak at 401.0 eV that is tentatively assigned to amine or NH containing heterocycles[27,28] (**Fig. 2**d). The 401.0 eV peak could be atmospheric N_2 which was either trapped in the inorganic phase or generated during X-ray exposure[28], but high $\delta^{15}N$ (shown below) in the matrix area indicate the presence of indigenous nitrogen compounds.

Fig. 3 shows high spatial resolution secondary ion mass spectrometry (NanoSIMS) isotope δD, $\delta^{15}N$ and $^{12}C^{14}N/^{16}O$ images of the FIB section containing the OM aggregate (same section shown in **Fig. 2**). Hydrogen, nitrogen and carbon isotopic and elemental ratios of the OM aggregate and surrounding matrix are summarized in **Table 1**. The OM aggregate had a large δD and $\delta^{15}N$ anomaly; δD = 2,370 ± 74 ‰ and $\delta^{15}N$ = 696 ± 100 ‰ on average. The $\delta^{13}C$ value was −43 ± 20 ‰ that was broadly consistent with the values of IOM from CR chondrites and the Bells meteorite (an unusual CM2 chondrite)[19] within analytical error. Two isotopic hot spots were observed; one is D- and ^{15}N-rich (δD = 4,200 ± 550 ‰ and $\delta^{15}N$ = 3,413 ± 1,070 ‰), and the other is D-rich (δD = 4,500 ± 900 ‰) and less ^{15}N-rich (724 ± 780 ‰) (Fig. 3e,f). These enrichments of the heavy isotopes suggest that the OM or its precursors formed by low-temperature chemistry in molecular clouds or the outer protosolar disk[29]. The origin of the

isotope heterogeneities (hot spots) in the OM aggregate in the Zag clast is puzzling since no molecular heterogeneity was observed between the hot spots and the average OM area (**Fig. 2**c).

N-XANES spectra and NanoSIMS $^{12}C^{14}N/^{16}O$ images of the Zag clast FIB section showed a relatively high concentration of nitrogen in the matrix region. A rough estimation by NanoSIMS for N/C elemental ratio of matrix was 0.036 ± 0.006 while N/C ratio of OM aggregate was 0.022 ± 0.003. The majority of carbon in the matrix comes from carbonates, therefore the N/C_{OM} ratio of the matrix would have been higher.

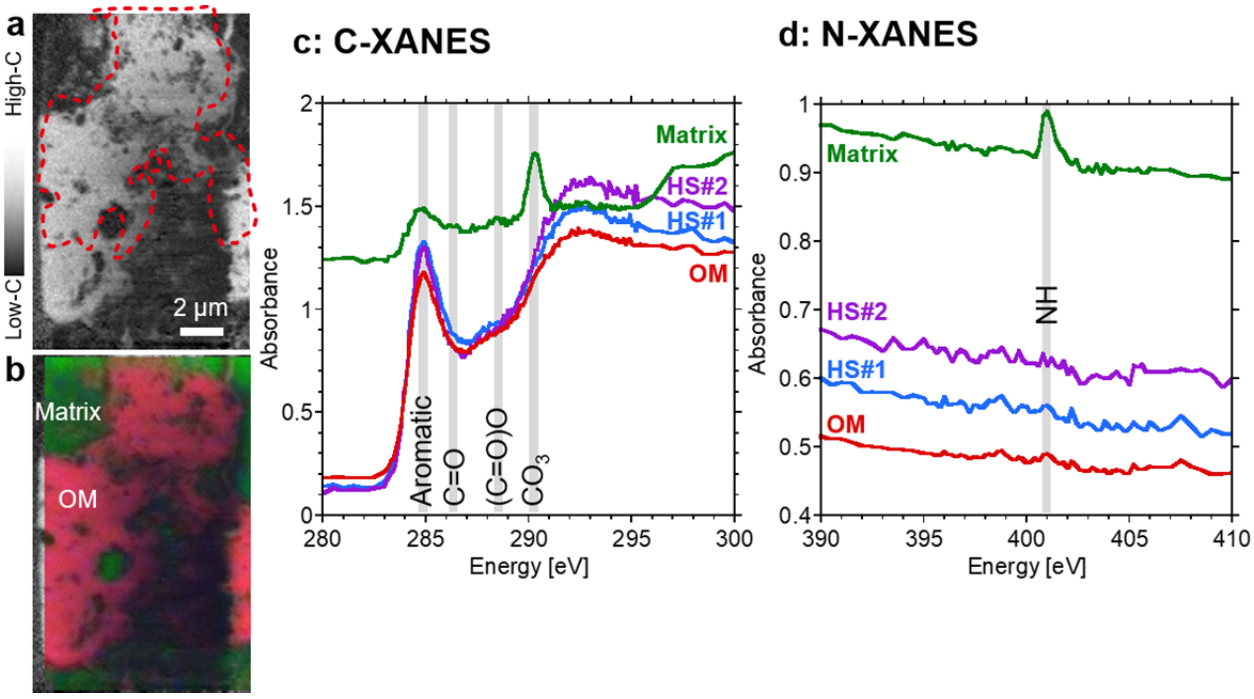

Fig. 2: Scanning transmission X-ray microscopy (STXM) analyses of a focused ion beam (FIB) section containing the organic matter (OM) aggregate in the Zag clast. (a) Carbon-map indicates the section is dominated by carbon. The location of the δD image (**Fig. 3**) is indicated by red dots. (b) Composition map derived from C-XANES of OM (red) and matrix (green). (c) Carbon X-ray absorption near-edge structure (C-XANES) of OM aggregate revealed that it is hydrogenated amorphous carbon (HAC)-like material dominated by sp^2 carbon (284.8

eV) while the surrounding matrix is mainly carbonates (290.3 eV) with some OM at 286.3 eV that is assigned to ketone (C=O) and 288.5 eV that is assigned to carboxyl/ester [(C=O)O]. (d) The OM aggregate does not show detectable N-XANES features while matrix shows a peak at 401.0 eV which is assigned to amine or NH in heterocycles. The C- and N-XANES obtained from isotope hot spots (HS, see **Fig. 3**) are also shown.

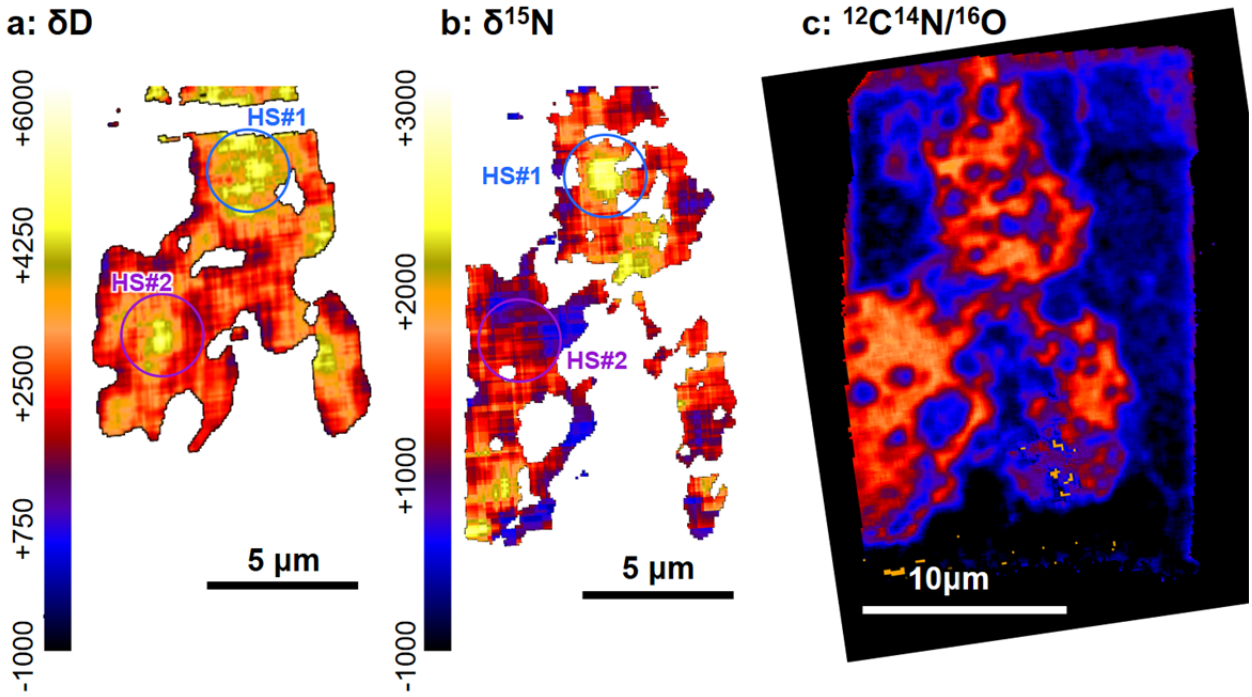

Fig. 3: NanoSIMS isotope images of the FIB section containing the organic matter (OM) aggregate in the Zag clast (same section with Fig. 2). (a) δD image (the location is indicated in red dots in **Fig. 2**a), (b) $\delta^{15}N$ image and (c) $^{12}C^{14}N/^{16}O$ ratio image. Isotopic hot spots are indicated by circles.

Table 1: Hydrogen, nitrogen and carbon isotopic and elemental ratios of organic matter (OM) aggregate and matrix of the Zag clast measured by NanoSIMS.

	δD ‰	δ^{15}N ‰	δ^{13}C ‰	H/C	N/C	O/C	O/C [a]
OM aggregate	2,370±74	696±100	−43±20	0.60±0.03	0.022±0.003	0.15±0.02	~0.06-0.07
Hot spot #1	4,200±550	3,413±1,070		0.41±0.02	0.032±0.006	0.16±0.02	
Hot spot #2	4,500±900	724±780					
Matrix	−	301±98	10±41		0.036±0.001		~1.4-1.6

[a] Estimated by C,N,O *K*-edge X-ray absorption spectra.

The large, micrometer-sized OM grains/aggregates are abundant in the Zag clast but are rare in other meteorites - a very few are known in CR chondrites[30,31]. The OM aggregate in the Zag clast studied here is somewhat similar to ultracarbonaceous Antarctic micrometeorites (UCAMM) that are considered as cometary materials[32], with respect to the size and the high concentrations of heavy isotopes (D and ^{15}N). However, C- and N-XANES analyses of UCAMM indicated the presence of O- and N-bearing functional groups, e.g., C=O, (C=O)O, C=N, and NHx(C=O)[33,34], that is not the case for the OM aggregate in the Zag clast. Cometary OM (CHON particles from comet Halley and returned samples from comet 81P/Wild 2) has higher H, N and O contents, compared to the OM aggregates[35,36]. The C-XANES spectra of comet 81P/Wild2 particles, as well as anhydrous and hydrated chondritic interplanetary dust particles and chondritic micrometeorites (some of which probably originated from comets) also show O-bearing functional groups (e.g., C=O at ~286.5 eV, (C=O)O at ~288.5 eV)[35,37-39].

The C-XANES spectrum of the OM aggregate does not resemble IOM in primitive CI/CM/CR chondrites that shows C=O at ~286.5 eV, (C=O)O at ~288.5 eV and sometime aliphatic carbon at ~287.5 eV[25]. Even the C-XANES spectra of the IOM from thermally-

157 metamorphosed chondrites (e.g., CV and CO chondrites and ordinary chondrites) have a 288.5
158 eV peak, in addition to 1s-σ* exciton at 291.7 eV indicating graphene structures[26], this is not the
159 case for the OM aggregate. A rough estimation for the O/C elemental ratio of the OM aggregate
160 from C,N,O X-ray absorption spectra is 0.06 to 0.07 (the method is reported elsewhere[35]), that is
161 lower than IOM extracted from CV, CO and ordinary chondrites[19]. The O/C ratio obtained by
162 NanoSIMS was 0.15, which can be attributed to uncertainty of O/C ratio obtained by
163 NanoSIMS[40].

164 C-XANES spectra of "aromatic" nanoglobules in chondrites reported by De Gregorio et
165 al.[41] are similar to the OM aggregate in the Zag clast. In their study, some aromatic nanoglobules
166 tend to have higher $\delta^{15}N$ values than IOM-like nanoglobules, although the correlation between
167 molecular structure and $\delta^{15}N$ was rather ambiguous[41]. The OM aggregate has isotopic
168 heterogeneities without molecular structure heterogeneities, and it indicates that the OM
169 aggregate consists of materials with different origins but which subsequently experienced similar
170 chemical evolution pathways. Note that we also found a globular OM grain in the Zag clast
171 (Extended Data Figure 1) but larger (~5 μm) than typical nanoglobules (<1 μm).

172 The high D/H and $^{15}N/^{14}N$ ratios suggest that the OM aggregate originated in a very cold
173 environment such as the interstellar medium or the outer region of the solar nebula. The OM
174 aggregate is in close proximity to the aqueously altered matrix, which indicates that the OM
175 aggregate was processed by the same aqueous event as the surrounding matrix. The low
176 temperature and extended period of the aqueous event could have reduced substituted functional
177 groups of the OM structure.

178 In the case of carbonaceous chondrites, significant decreases in D/H ratio of OM are
179 accompanied by aqueous alteration mostly due to D-H exchange with D-poor water, e.g., the δD

value of OM in the most aqueously altered CI chondrites is ~970-980 ‰ in contrast to the high δD values of the least altered carbonaceous chondritic OM (up to ~3500 ‰)[19]. If this is the case of the Zag clast, the D/H ratio of the OM is expected to be reduced during the heavy aqueous alteration reflected in the mineralogy of the clast, i.e., CI chondrite like compositions[10,11]. Therefore, D-rich water is required to maintain the high D/H ratio (δD ~ 2400 ‰) in the OM aggregate, such as the water in Enceladus which has a D/H ratio of $2.9\ (+1.5/-0.7) \times 10^{-4}$ (δD ~ 1820 to 410 ‰)[20]. Water in halite, which has plausibly the same origin as water in the clast, shows a large variation of δD, −400 to +1300 ‰, and it is attributed to the variation in degree of water-rock interactions[42].

The surrounding matrix contains N-rich compounds possibly in the form of amine or heterocycles. These N-bearing compounds would not share the same origin with the OM aggregate since the $\delta^{15}N$ value of the OM is ~700 ± 100 ‰ while the matrix is ~300 ± 100 ‰. IOM in carbonaceous chondrites is known to release ammonia up to 10 μg/mg via hydrothermal processing at 300–400 °C, but the $\delta^{15}N$ of the released fractions are higher than the original IOM[43]. In any case, N-rich compounds and carbonates in the matrix of the Zag clast is consistent with recent observation of ammoniated phyllosilicates and carbonates in the regolith of Ceres[21,23,44].

The recent discovery of ammoniated phyllosilicates on the surface of Ceres implies that material from the outer Solar System was incorporated into Ceres, either during its formation at great heliocentric distance or by incorporation of material transported into the main asteroid belt [21]. This is consistent with the high D/H and $^{15}N/^{14}N$ ratios of the OM aggregate as well as the observed extensive parent body aqueous alteration involving D-rich water. Our results further support the idea that Ceres originated in the outer region of the Solar System, then migrated

inward to the main belt region scattered by migrations of Jupiter and Saturn as required by the "Grand Tack" scenario[21,22]. Ceres could have originated as a salty ocean world similar to Enceladus[45] and was subsequently transported to the main belt region where the icy ocean sublimated to leave behind salts, carbonates, clays and organic matter.

Acknowledgements

This work is supported by the Astrobiology Center Program of National Institutes of Natural Sciences (NINS) (Grant Number AB281004), and the NASA Hayabusa2 Participating Scientist Program (MEZ).

Methods

Sample preparation using a focused ion beam (FIB)

The OM aggregate was selected from a polished thin section of the xenolithic clast in the Zag meteorite using imaging from a JEOL 7600F field emission gun scanning electron microscope (FEG-SEM) at NASA/JSC. Approximately 100 nm-thick sections were subsampled from the OM aggregate in the Zag clast using a Quanta 3d FEG focused ion beam (FIB) instrument at NASA/JSC.

Scanning-Transmission X-ray Microscopy (STXM)

Carbon, nitrogen and oxygen X-ray absorption near edge structure (C,N,O-XANES) micro-spectroscopy was performed using the scanning-transmission X-ray microscopes (STXM) at BL13A of the Photon Factory, High Energy Accelerator Research Organization (KEK)[46,47]. The carbon map was obtained by acquiring pairs of images below and on the carbon *K*-edge, at 280 and 292 eV, respectively, and taking the $-\ln(I_{292}/I_{280})$ for each pixel. The C-XANES spectra were acquired with the energy step sizes (ΔE) of 0.1 eV in 283–295.5 eV region, 0.5 eV in 280–283 eV and 295.5–301.0 eV regions, and 1 eV in 301–310 eV region. For N-XANES, ΔE was 0.2 eV in 395–406 eV region, 0.5 eV in 385–395 eV and 406–410 eV regions, and 2 eV in 410–430 eV region. For O-XANES, ΔE was 0.2 eV in 530–540 eV region, 1 eV in 520–530 eV and 540–560 eV regions, and 2 eV in 560–580 eV region. The acquisition time per energy step was 5 to 10 ms.

NanoSIMS ion microprobe

H, C and N isotope imaging measurements of the Zag clast FIB section were carried out with the JAMSTEC NanoSIMS 50L. Detailed measurement conditions are described elsewhere[48,49]. Briefly, a focused Cs^+ primary ion beam of 0.8 to 4 pA was rastered over 25 μm x 25 μm areas on the sample and a standard material (1-hydroxybenzotriazole hydrate; $C_6H_5N_3O \cdot \mathbf{x}H_2O$, calculated as x=1). The spatial resolution was estimated to be ~100 nm for C and N isotope images, and ~200 nm for H isotope image. Each run repeatedly scanned (10 to 20 times) over the same area. Individual images consist of 256 x 256 pixels with acquisition time of 6,000 μs/pixel (393 sec/frame) for C and N isotope images, and of 5,000 μs/pixel (328 sec/frame) for H isotope image. Each measurement was started after stabilization of the secondary ion intensities following a pre-sputtering procedure of approximately 1–3 min. The sample was coated with a 10 nm Au thin film to mitigate electrostatic charge on the surface. During the analysis, the mass peaks were centered automatically every 5 cycles.

References

1 Rubin, A. E., Zolensky, M. E. & Bodnar, R. J. The halite‐bearing Zag and Monahans (1998) meteorite breccias: Shock metamorphism, thermal metamorphism and aqueous alteration on the H‐chondrite parent body. *Meteoritics & Planetary Science* **37**, 125-141 (2002).

2 Brearley, A. J. Carbon-rich aggregates in type 3 ordinary chondrites: Characterization, origins, and thermal history. *Geochimica et Cosmochimica Acta* **54**, 831-850, doi:10.1016/0016-7037(90)90377-W (1990).

3 Buchanan, P., Zolensky, M. & Reid, A. Carbonaceous chondrite clasts in the howardites Bholghati and EET87513. *Meteoritics* **28**, 659-669 (1993).

4 Zolensky, M. *et al.* Mineralogy, petrology and geochemistry of carbonaceous chondritic clasts in the LEW 85300 polymict eucrite. *Meteoritics* **27**, 596-604 (1992).

5 Zolensky, M. E. Asteroidal Water Within Fluid Inclusion-Bearing Halite in an H5 Chondrite, Monahans (1998). *Science* **285**, 1377-1379, doi:10.1126/science.285.5432.1377 (1999).

6 Zolensky, M. E., Weisberg, M. K., Buchanan, P. C. & Mittlefehldt, D. W. Mineralogy of carbonaceous chondrite clasts in HED achondrites and the Moon. *Meteoritics & Planetary Science* **31**, 518-537 (1996).
7 Nakashima, D., Nakamura, T. & Noguchi, T. Formation history of CI-like phyllosilicate-rich clasts in the Tsukuba meteorite inferred from mineralogy and noble gas signatures. *Earth and Planetary Science Letters* **212**, 321-336 (2003).
8 Brearley, A. J. CI chondrite-like clasts in the Nilpena polymict ureilite: Implications for aqueous alteration processes in CI chondrites. *Geochimica et Cosmochimica Acta* **56**, 1373-1386 (1992).
9 Fries, M., Messenger, S., Steele, A. & Zolensky, M. Do We Already have Samples of Ceres? H Chondrite Halites and the Ceres-Hebe Link. *76th Annual Meeting of the Meteoritical Society*, Abstract #5266 (2013).
10 Zolensky, M. *et al.* The Mineralogy of Ceres*(* Or Something an Awful Lot Like It). *78th Annual Meeting of the Meteoritical Society*, Abstract #5270 (2015).
11 Zolensky, M. E. *et al.* The search for and analysis of direct samples of early Solar System aqueous fluids. *Philosophical Transactions of the Royal Society A: Mathematical, Physical and Engineering Sciences* **375**, doi:10.1098/rsta.2015.0386 (2017).
12 Fries, M., Zolensky, M. & Steele, A. Mineral inclusions in Monahans and Zag halites: Evidence of the originating body. *Meteoritics and Planetary Science Supplement* **74** (2011).
13 Robertson, J. Hard amorphous (diamond-like) carbons. *Progress in Solid State Chemistry* **21**, 199-333 (1991).
14 Ray, S. C. *et al.* Studies of ion irradiation effects in hydrogenated amorphous carbon thin films by X-ray absorption and photoemission spectroscopy. *Thin Solid Films* **516**, 3374-3377, doi:10.1016/j.tsf.2007.10.020 (2008).
15 Buijnsters, J. G. *et al.* Hydrogen quantification in hydrogenated amorphous carbon films by infrared, Raman, and x-ray absorption near edge spectroscopies. *Journal of Applied Physics* **105**, doi:10.1063/1.3103326 (2009).
16 Buijnsters, J. G., Gago, R., Redondo-Cubero, A. & Jimenez, I. Hydrogen stability in hydrogenated amorphous carbon films with polymer-like and diamond-like structure. *Journal of Applied Physics* **112**, doi:10.1063/1.4764001 (2012).
17 Tunmee, S. *et al.* Study of Synchrotron Radiation Near-Edge X-Ray Absorption Fine-Structure of Amorphous Hydrogenated Carbon Films at Various Thicknesses. *Journal of Nanomaterials*, doi:10.1155/2015/276790 (2015).
18 Jia, L. Y. *et al.* Effect of gas residence time on near-edge X-ray absorption fine structures of hydrogenated amorphous carbon films grown by plasma-enhanced chemical vapor deposition. *Japanese Journal of Applied Physics* **55**, doi:10.7567/jjap.55.040305 (2016).
19 Alexander, C. M. O. D., Fogel, M., Yabuta, H. & Cody, G. D. The origin and evolution of chondrites recorded in the elemental and isotopic compositions of their macromolecular organic matter. *Geochimica et Cosmochimica Acta* **71**, 4380-4403, doi:10.1016/j.gca.2007.06.052 (2007).
20 Waite Jr, J. H. *et al.* Liquid water on Enceladus from observations of ammonia and 40Ar in the plume. *Nature* **460**, 487-490, doi:http://www.nature.com/nature/journal/v460/n7254/suppinfo/nature08153_S1.html (2009).

21 De Sanctis, M. C. *et al.* Ammoniated phyllosilicates with a likely outer Solar System origin on (1) Ceres. *Nature* **528**, 241-244, doi:10.1038/nature16172 (2015).

22 Walsh, K. J., Morbidelli, A., Raymond, S. N., O'Brien, D. P. & Mandell, A. M. A low mass for Mars from Jupiter/'s early gas-driven migration. *Nature* **475**, 206-209 (2011).

23 McSween, H. Y. *et al.* Carbonaceous chondrites as analogs for the composition and alteration of Ceres. *Meteoritics & Planetary Science* **in press**, doi:10.1111/maps.12947 (2017).

24 Gaffey, M. J. & Gilbert, S. L. Asteroid 6 Hebe: The probable parent body of the H‐type ordinary chondrites and the IIE iron meteorites. *Meteoritics & Planetary Science* **33**, 1281-1295, doi:10.1111/j.1945-5100.1998.tb01312.x (1998).

25 Le Guillou, C., Bernard, S., Brearley, A. J. & Remusat, L. Evolution of organic matter in Orgueil, Murchison and Renazzo during parent body aqueous alteration: In situ investigations. *Geochimica et Cosmochimica Acta* **131**, 368-392, doi:10.1016/j.gca.2013.11.020 (2014).

26 Cody, G. D. *et al.* Organic thermometry for chondritic parent bodies. *Earth and Planetary Science Letters* **272**, 446-455, doi:10.1016/j.epsl.2008.05.008 (2008).

27 Newbury, D., Ishii, I. & Hitchcock, A. Inner shell electron-energy loss spectroscopy of some heterocyclic molecules. *Canadian Journal of Chemistry* **64**, 1145-1155 (1986).

28 Leinweber, P. *et al.* Nitrogen K-edge XANES - an overview of reference compounds used to identify `unknown' organic nitrogen in environmental samples. *Journal of Synchrotron Radiation* **14**, 500-511, doi:doi:10.1107/S0909049507042513 (2007).

29 Yang, J. & Epstein, S. Interstellar organic-matter in meteorites. *Geochimica et Cosmochimica Acta* **47**, 2199-2216, doi:10.1016/0016-7037(83)90043-1 (1983).

30 Peeters, Z., Changela, H., Stroud, R., Alexander, C. & Nittler, L. in *Lunar and Planetary Science Conference.*

31 J. Leitner, C. V., P. Hoppe. A SEM AND NANOSIMS INVESTIGATION OF ORGANIC AGGREGATES IN THE CR CHONDRITES MILLER RANGE 07525 AND RENAZZO. *80th Annual Meeting of the Meteoritical Society 2017 (LPI Contrib. No. 1987)* (2017).

32 Duprat, J. *et al.* Extreme deuterium excesses in ultracarbonaceous micrometeorites from central Antarctic snow. *Science* **328**, 742-745, doi:10.1126/science.1184832 (2010).

33 Engrand, C. *et al.* in *Lunar and Planetary Science Conference.* 1902.

34 Yabuta, H. *et al.* Formation of an ultracarbonaceous Antarctic micrometeorite through minimal aqueous alteration in a small porous icy body. *Geochimica et Cosmochimica Acta* **214**, 172-190, doi:https://doi.org/10.1016/j.gca.2017.06.047 (2017).

35 Cody, G. D. *et al.* Quantitative organic and light-element analysis of comet 81P/Wild 2 particles using C-, N-, and O-μ-XANES. *Meteoritics & Planetary Science* **43**, 353-365 (2008).

36 Kissel, J. & Krueger, F. The organic component in dust from comet Halley as measured by the PUMA mass spectrometer on board Vega 1. *Nature* **326**, 755-760 (1987).

37 Flynn, G. J., Keller, L. P., Feser, M., Wirick, S. & Jacobsen, C. The origin of organic matter in the solar system: Evidence from the interplanetary dust particles. *Geochimica et Cosmochimica Acta* **67**, 4791-4806, doi:10.1016/j.gca.2003.09.001 (2003).

38 Keller, L. P. *et al.* The nature of molecular cloud material in interplanetary dust. *Geochimica et Cosmochimica Acta* **68**, 2577-2589, doi:10.1016/j.gca.2003.10.044 (2004).

39 Noguchi, T. *et al.* Variation of mineralogy and organic material during the early stages of aqueous activity recorded in Antarctic micrometeorites. *Geochimica et Cosmochimica Acta* **208**, 119-144, doi:10.1016/j.gca.2017.03.034 (2017).
40 Alleon, J., Bernard, S., Remusat, L. & Robert, F. Estimation of nitrogen-to-carbon ratios of organics and carbon materials at the submicrometer scale. *Carbon* **84**, 290-298, doi:10.1016/j.carbon.2014.11.044 (2015).
41 De Gregorio, B. T. *et al.* Isotopic and chemical variation of organic nanoglobules in primitive meteorites. *Meteoritics & Planetary Science* **48**, 904-928, doi:10.1111/maps.12109 (2013).
42 Yurimoto, H. *et al.* Isotopic compositions of asteroidal liquid water trapped in fluid inclusions of chondrites. *Geochemical Journal* **48**, 549-560, doi:10.2343/geochemj.2.0335 (2014).
43 Pizzarello, S. & Williams, L. B. Ammonia in the early Solar System: An account from carbonaceous meteorites. *The Astrophysical Journal* **749**, 161, doi:10.1088/0004-637x/749/2/161 (2012).
44 De Sanctis, M. C. *et al.* Bright carbonate deposits as evidence of aqueous alteration on (1) Ceres. *Nature* **536**, 54-57, doi:10.1038/nature18290 (2016).
45 Postberg, F. *et al.* Sodium salts in E-ring ice grains from an ocean below the surface of Enceladus. *Nature* **459**, 1098-1101, doi:http://www.nature.com/nature/journal/v459/n7250/suppinfo/nature08046_S1.html (2009).
46 Takeichi, Y., Inami, N., Suga, H., Ono, K. & Takahashi, Y. Development of a compact scanning transmission X-ray microscope (STXM) at the photon factory. *Chemistry Letters* **43**, 373-375 (2014).
47 Takeichi, Y. *et al.* Design and performance of a compact scanning transmission X-ray microscope at the Photon Factory. *Review of Scientific Instruments* **87**, 013704 (2016).
48 Ito, M. & Messenger, S. Isotopic imaging of refractory inclusions in meteorites with the NanoSIMS 50L. *Applied Surface Science* **255**, 1446-1450, doi:10.1016/j.apsusc.2008.05.095 (2008).
49 Ito, M. *et al.* H, C, and N isotopic compositions of Hayabusa category 3 organic samples. *Earth, Planets and Space* **66**, 91, doi:10.1186/1880-5981-66-91 (2014).

Extended Data

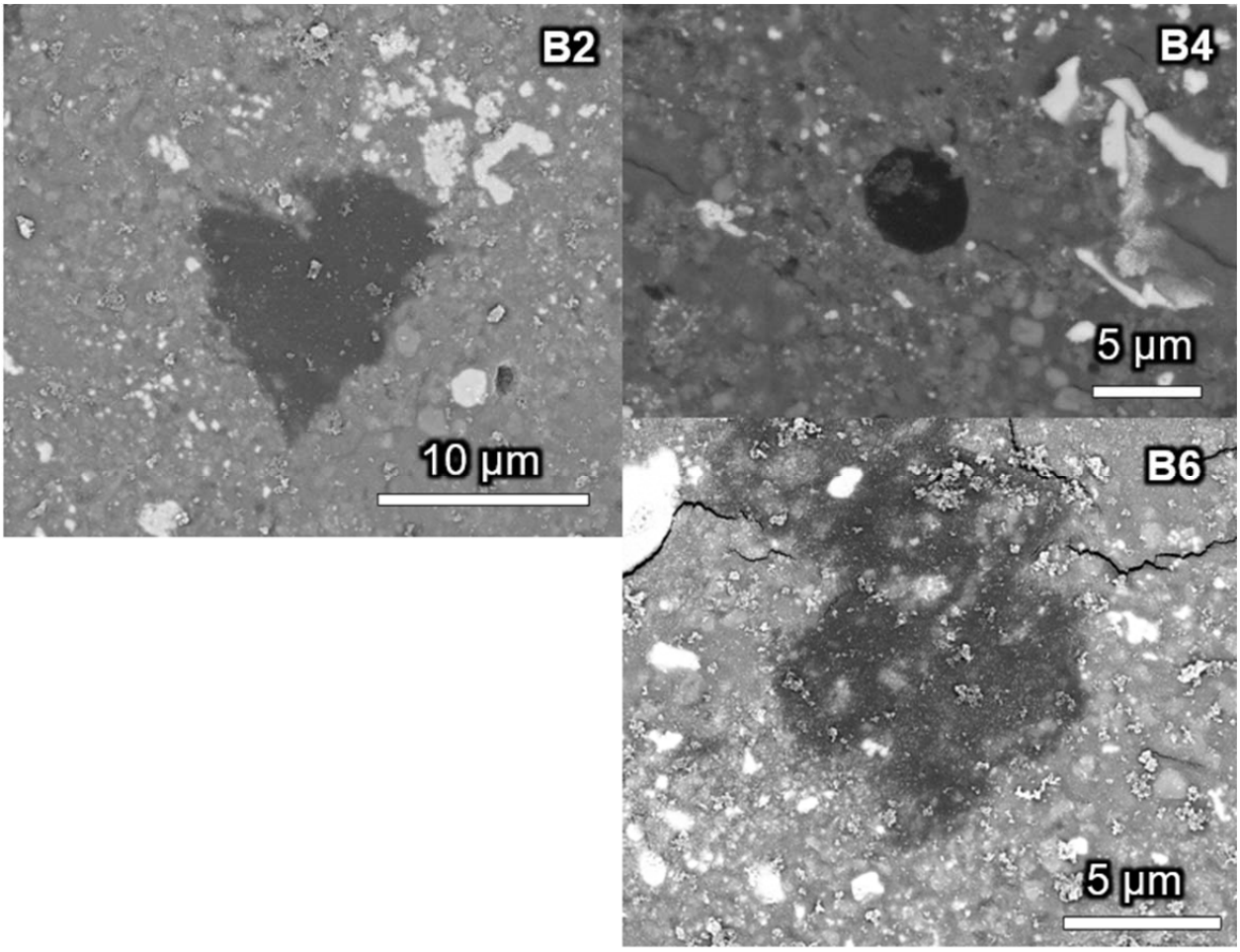

Extended Data Figure 1: **Backscattered electron images (BEI) of organic grains/aggregates (black) in the clast in the Zag clast.**

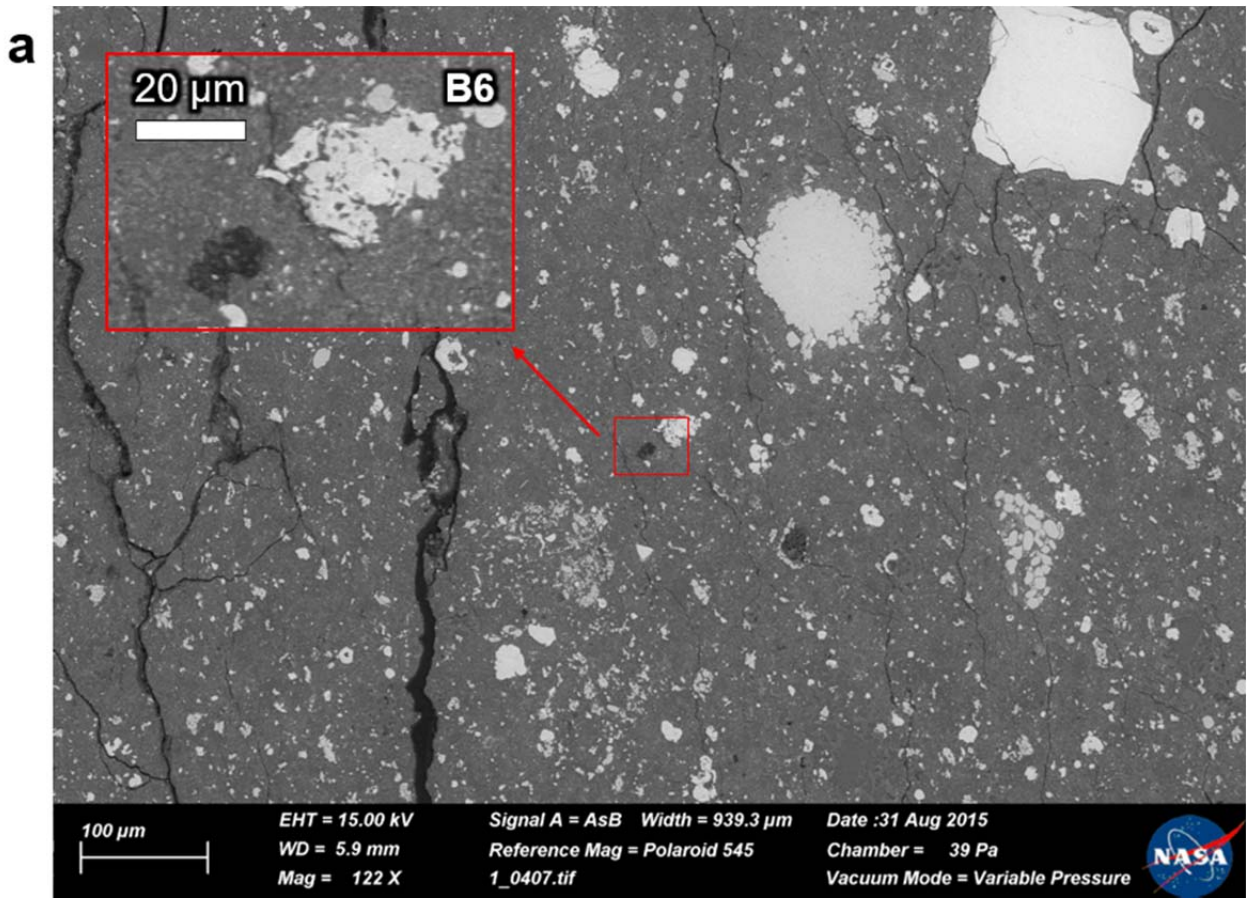
a
20 µm
B6
100 µm
EHT = 15.00 kV
WD = 5.9 mm
Mag = 122 X
Signal A = AsB Width = 939.3 µm
Reference Mag = Polaroid 545
1_0407.tif
Date :31 Aug 2015
Chamber = 39 Pa
Vacuum Mode = Variable Pressure
NASA

399

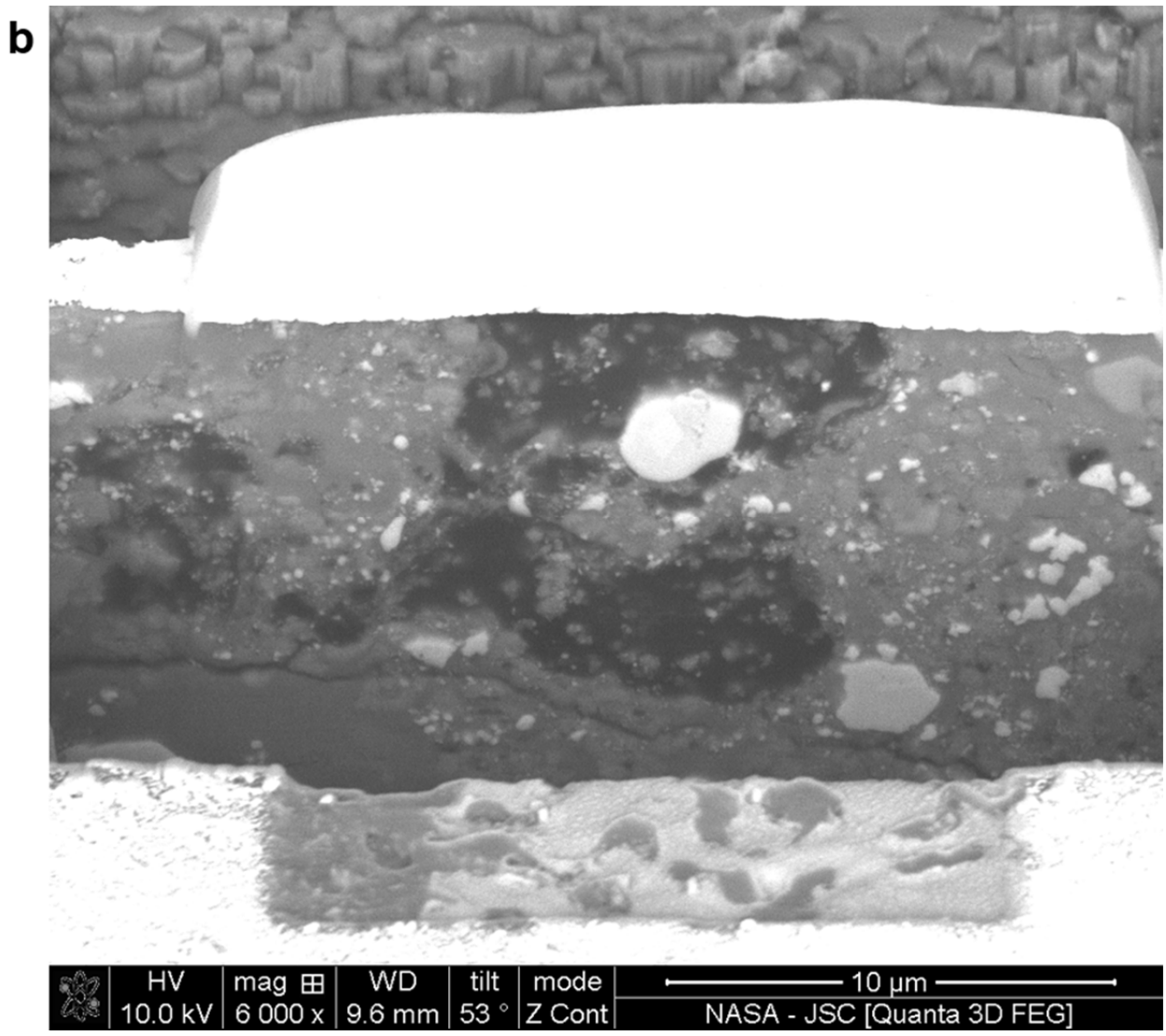

Extended Data Figure 2: **Images of before and during sample preparation.** (a) Backscatter electron image of the clast from the Zag meteorite. The OM aggregate analyzed here is shown in red squares. (b) Backscatter electron image of the focused ion beam (FIB) section from the OM aggregate in the Zag clast during the FIB milling process.

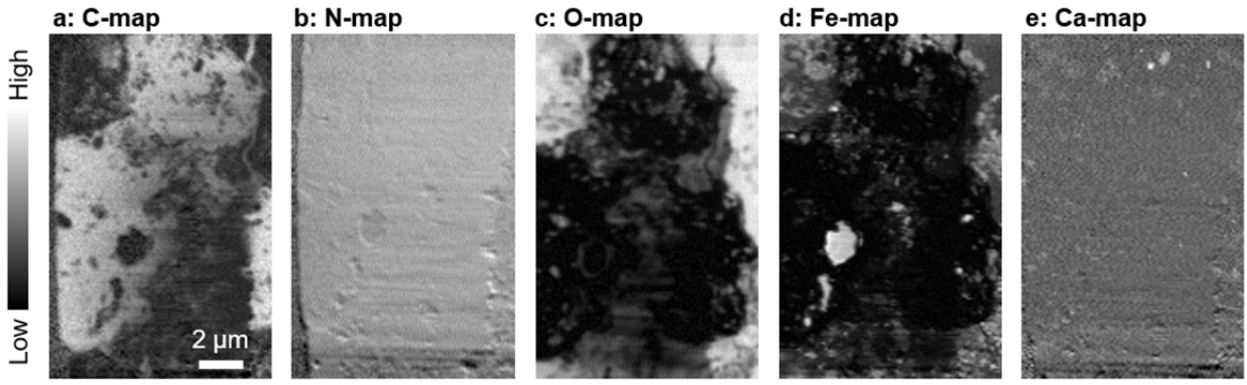

406

407 Extended Data Figure 3: **STXM elemental map of the FIB section including the OM**
408 **aggregates in the Zag clast.** (a) C-map: $-\ln(I_{292}/I_{280})$, (b) N-map: $-\ln(I_{405}/I_{395})$, (c) O-map: –
409 $\ln(I_{539}/I_{525})$, (d) Fe-map: $-\ln(I_{709}/I_{705})$, and (e) Ca-map: $-\ln(I_{349}/I_{345})$.

410

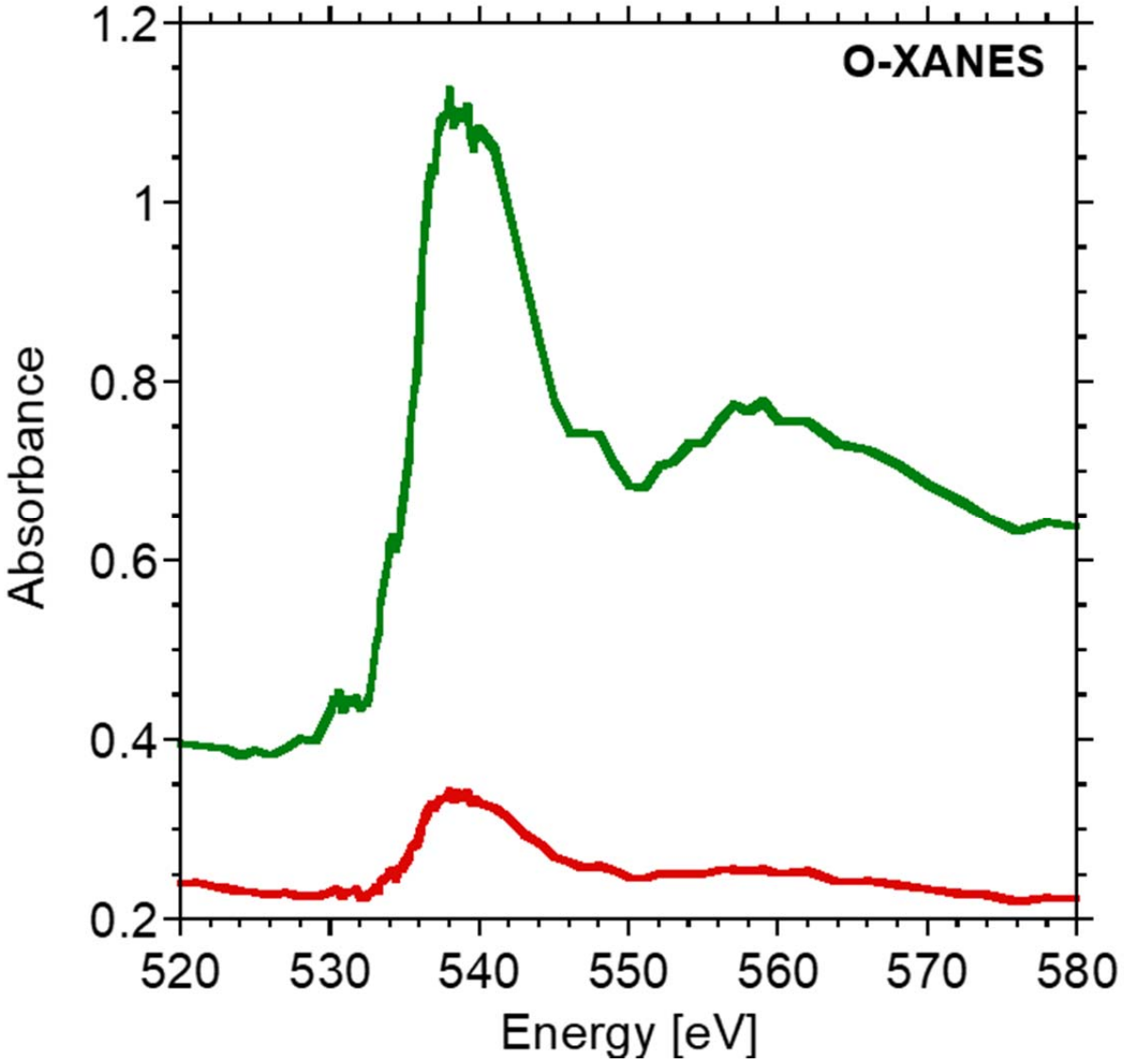

411

412 Extended Data Figure 4: **O-XANES spectra of the Zag clast.** The OM aggregate is shown in
413 red, and surrounding matrix is in green.

414

415